Addressing NHS Chemistry: Efficient Quenching of Excess TMT Reagent and Reversing TMT Overlabeling in Proteomic Samples by Methylamine

Authors

Yana Demyanenko, Xintong Sui, Andrew M. Giltrap, Benjamin G. Davis, Bernhard Kuster, and Shabaz Mohammed

Correspondence

shabaz.mohammed@rfi.ac.uk

In Brief

N-hydroxysuccinimide (NHS) ester chemistry is used extensively across proteomics sample preparation. However, the role of NHS esters as activated carboxyls can also drive the formation of serine-, tyrosine-, and threonine-derived esters (*O*-derivatives). Their presence also unnecessarily increases sample complexity, which reduces the overall identification rates. We have now developed a robust method, using methylamine, to efficiently remove overlabeled peptides. Overlabeling is reduced to lower than 1% leading to superior identification rates and quantitation precision.

Graphical Abstract

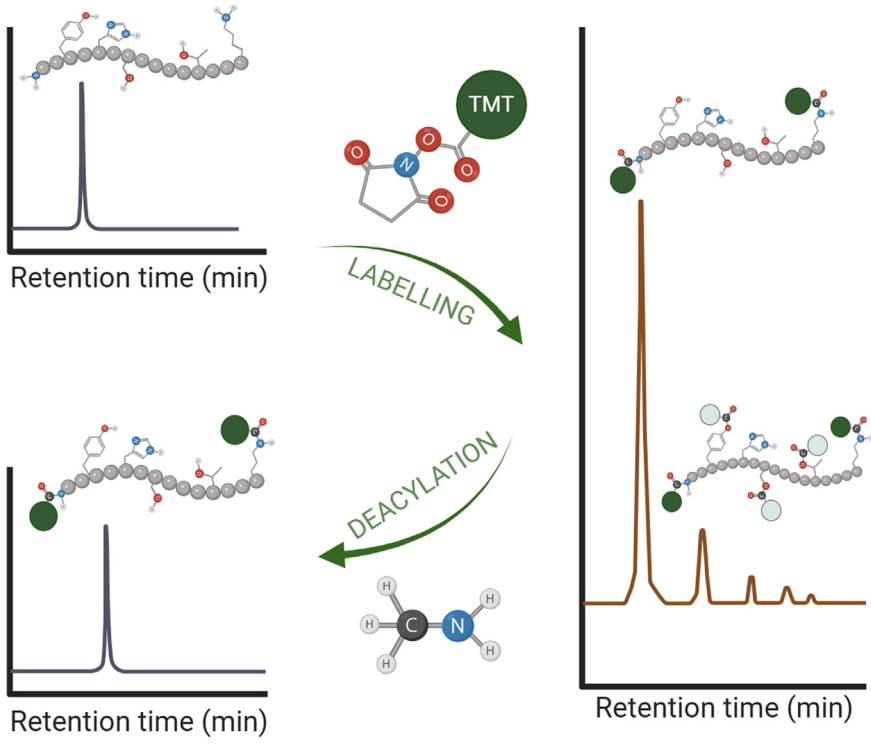

2025, Mol Cell Proteomics *24*(*4*), 100948

https://doi.org/10.1016/j.mcpro.2025.100948

Highlights

- Methylamine is superior to hydroxylamine for reversal of overlabeling.
- Robust cleavage of *N*-hydroxysuccinimide-labeling byproducts for all three main O-acyl esters: serine, threonine, and tyrosine.
- Methylamine improves signal and identification rates in tandem mass tag–based proteomics and phosphoproteomics experiments.
- The method can be easily inserted into existing *N*-hydroxysuccinimide-labeling protocols.

Addressing NHS Chemistry: Efficient Quenching of Excess TMT Reagent and Reversing TMT Overlabeling in Proteomic Samples by Methylamine

Yana Demyanenko[1,2], Xintong Sui[3], Andrew M. Giltrap[1,2,4], Benjamin G. Davis[1,2,4], Bernhard Kuster[3], and Shabaz Mohammed[1,4,5,*]

***N*-hydroxysuccinimide (NHS) ester chemistry is used extensively across proteomics sample preparation. One of its increasingly prevalent applications is in isobaric reagent–based quantitation such as isobaric tags for relative and absolute quantitation and tandem mass tag approaches. In these methods, labeling on the primary amines of lysine residues and N termini of tryptic peptides *via* amide formation (*N*-derivatives) from corresponding NHS ester reagents is the intended reactive outcome. However, the role of NHS esters as activated carboxyls can also drive the formation of serine-, tyrosine-, and threonine-derived esters (*O*-derivatives). These *O*-derivative peptides are typically classed as overlabeled and are disregarded for quantitation, leading to loss of information and hence potential sensitivity. Their presence also unnecessarily increases sample complexity, which reduces the overall identification rates. One common approach for removing these unwanted labeling events has involved treatment with hydroxylamine. We show here that this approach is not efficient and can still leave substantial levels of unwanted overlabeled peptides. Through systematic study of nucleophilic aminolysis reagents and reaction conditions, we have now developed a robust method to efficiently remove overlabeled peptides. The new method reduces the proportion of overlabeled peptides in the sample to less than 1% without affecting the labeling rate or introducing other modifications, leading to superior identification rates and quantitation precision.**

N-hydroxysuccinimide (NHS)-activated ester compounds were originally developed for peptide synthesis under diverse, including aqueous, conditions (1). They are highly reactive carboxyl derivatives, and when applied to proteins, they show some selectivity toward primary amines of N termini and N_{ε} of lysines (2–4); reversible reactions with disulfides and hydroxyl groups of tyrosines have been suggested (5–7). NHS esters have therefore found widespread use in a range of biochemical applications including, for instance, covalent modifications for enzyme activation (5, 8), biotinylation for hybridization and detection (9–11), heavy metal and fluorescent labeling for imaging and structure elucidation (2, 12).

In the proteomics field, NHS esters are used as crosslinking reagents for protein network analysis and structure elucidation (13–15) as well as to introduce stable isotope labels to tryptic peptides for quantitation (16, 17). Specifically, tandem mass tags (TMTs) (17) and isobaric tags for relative and absolute quantitation (16) have been developed to allow quantitation of multiple samples in a single run, thereby minimizing impact of technical variation. Both reagent types rely on NHS ester chemistry to attach isotopically coded groups to N termini and lysines of tryptic peptides of each sample before combining them for analysis. These modifications result in the same nominal addition to the precursor mass across all conditions but release a differential reporter ion upon collision-induced dissociation, which provides quantitative information. As the samples are mixed prior to analysis, complete labeling and robust quenching are paramount to precision of quantitation using this method.

The NHS ester labeling reaction at most N termini and lysine ϵ-amines as reactive nucleophiles is considered to be most efficient at pH 8.0 to 9.0, under conditions where certain side products, such as tyrosyl esters, are formed and hydrolyzed (7). At this pH, the rate of concurrent NHS ester hydrolysis also increases and so is in competition with the desired amide

From the [1]The Rosalind Franklin Institute, Harwell, UK; [2]Department of Pharmacology, University of Oxford, Oxford, UK; [3]Chair of Proteomics and Bioanalytics, Technical University of Munich, Freising, Germany; [4]Chemistry Research Laboratory, Department of Chemistry, University of Oxford, Oxford, UK; [5]Department of Biochemistry, University of Oxford, Oxford, UK

*For correspondence: Shabaz Mohammed, shabaz.mohammed@rfi.ac.uk.

Present address for Andrew M. Giltrap: School of Mathematical and Physical Sciences, Faculty of Science, University of Technology Sydney, Ultimo NSW 2007, Australia.

https://doi.org/10.1016/j.mcpro.2025.100948

labeling reaction. Together with slight differences in individual reaction kinetics because of the local environments of nucleophiles on peptides, small changes in reaction conditions can lead to incomplete and/or heterogeneous labeling (18). As a result, peptide concentration, reaction pH, and water content have been optimized under most current protocols to achieve >99% labeling efficiency and minimize side-product formation (19). However, under these conditions, it has been shown that alongside tyrosines, serines and threonines can also be labeled though *O*-acylation of their hydroxyl groups to form ester *O*-derivative, especially when located in proximity to histidines (20–23) which may act as internal relay residues or general bases (Fig. 1). Together, these amino acids (Ser, Thr, Tyr, and STY) comprise over 15% of the proteome and so are similar in abundance to primary amines in the sample. As *O*-acylation reaction is typically slower than *N*-acylation under the conditions required for complete *N*-acylation of primary amines, a lower proportion of these hydroxyl groups is thus labeled. This leads to generation of several forms of each STY-containing peptide, each with a different number of tags (22). Moreover, where there are multiple hydroxyl residues on the same peptide, *O*-acylation is likely to occur only on one or two such residues with sequence-dependent likelihood for each residue, which may translate into differential chromatographic retention.

Regardless of origin, multiple versions of the same peptide unnecessarily increase sample complexity and lead to wasted time during data-dependent acquisition. The strong dependence of *O*-acylation prevalence on exact reaction conditions may lead to increased variation and therefore decreased quantitation precision where reaction volume, pH, and peptide or solvent concentration cannot be sufficiently controlled between samples. These issues have been recognized by the community, and solutions have been sought. As *O*-acyl esters are less stable than the amide bonds generated through *N*-acylation of primary amines, it is potentially possible to selectively reverse *O*-acyl formation by employing an appropriate nucleophile. Hydroxylamine treatment was shown to reverse tyrosyl ester formation on model peptides and has since been universally applied as a dual purpose reagent, which is to quench the excess of TMT reagent and reverse *O*-acylation (22). However, like others before us, we have found that overlabeled peptides are still present in samples labeled and quenched with the standard protocol and lead to systematic under-representation of STY-containing peptides in TMT datasets (19, 24). Several alternative approaches have been proposed to further reduce the abundance of *O*-acyl esters in TMT-labeled samples. A selection of commonly used labeling and aminolysis conditions can be found in Supplemental Table S1. For example, raised temperature increases hydrolysis of *O*-acyl esters at high pH without introducing additional reagents. Thus, boiling of samples for 1 h has been shown to reduce *O*-acylation in TMT-labeled samples (25). Alternatively, others have proposed that there is reduced *O*-acyl ester formation when performing the labeling reaction at pH 6.7 (24, 26). However, under these conditions, the rate of *N*-acylation is also reduced; therefore, complete labeling in solution requires higher temperature, excess of the labeling reagent, and further reduced water content (24). Whilst complete labeling at low pH can be achieved using reduced TMT reagent to peptide ratio under controlled conditions, higher ratios are recommended for robust labeling in

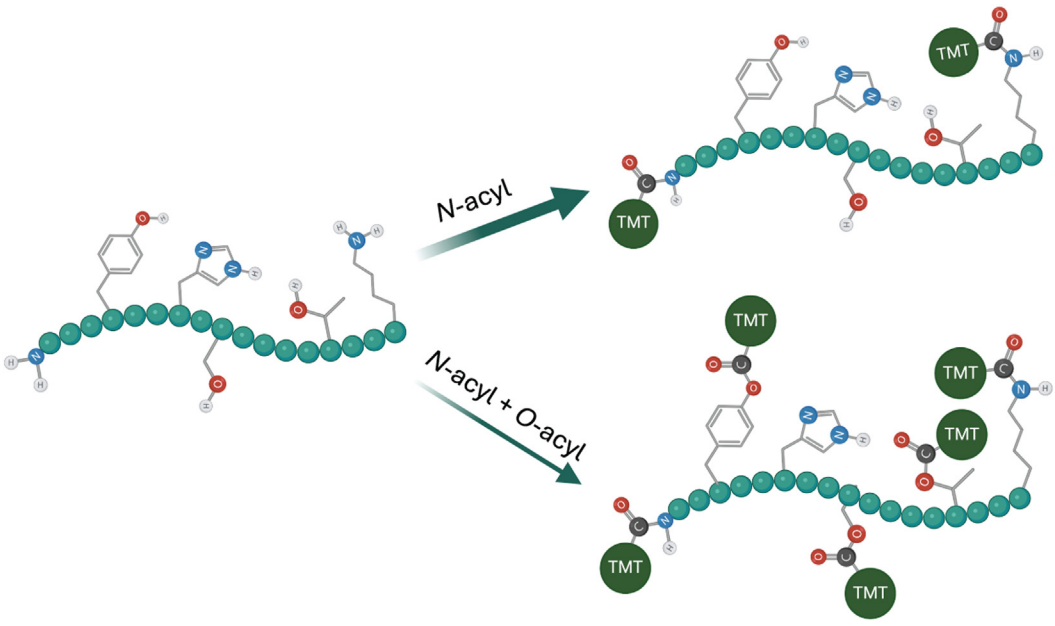

Fig. 1. **A schematic representation of potential products of peptide labeling with TMT reagent.** TMT, tandem mass tag.

real quantitative experiments (27). As NHS ester compounds, including TMT reagents, have been in use for decades, protocols for complete labeling of peptides have been optimized for many types of applications, including single-cell protein quantitation (28) and automated workflows (29–32). Required boiling of samples or change of pH between the digestion and labeling steps through desalting, drying, and resuspension can introduce additional sample losses and variation and may not be viable for some applications.

Here, through the reconsideration of the fundamental deacylation chemistries that may be selectively applied to unwanted *O*-derivatives, we have re-examined the strategy of cleavage postlabeling. The resulting discovery of the additional more efficient nucleophiles for this "clean-up" of NHS-labeling reactions substantially reduces *O*-acylation with minimal protocol changes.

EXPERIMENTAL PROCEDURES

Expi293F Lysate Preparation and Protein Digestion

Expi293 (human cell line based on human embryonic kidney 293) cell pellet was resuspended in lysis buffer (2% SDS [Sigma–Aldrich], 50 mM triethylamine bicarbonate (TEAB) [Supelco]), and sonicated using Bioruptor Pico (Diagenode) for 30 cycles (30 s on/off). Protein concentration was determined using bicinchoninic acid assay (Thermo Fisher Scientific) following the manufacturer's protocol prior to reduction and alkylation with 10 mM Tris(2-carboxyethyl) phosphine (Thermo Fisher) and 50 mM chloroacetamide (Sigma–Aldrich) for 30 min. Proteins were then digested using a modified single-pot solid phase–assisted sample preparation method (SP3) (33, 34) using magnetic carboxyl-coated magnetic beads (Cytiva) at 4:1 w/w ratio. Proteins were precipitated onto the beads using acetonitrile (ACN; 80% final concentration) and incubated for 30 min with shaking. Once proteins were immobilized, the beads were washed three times with 80% ethanol, followed by three washes with 100% ACN before incubation with digestion buffer (50 mM TEAB, containing sequencing-grade trypsin [Promega]) at 1:25 enzyme-to-protein ratio for 4 h. Supernatant was collected, and beads were washed with 2% dimethyl sulfoxide (DMSO) solution and combined with supernatant before acidification with formic acid (FA; 5% final concentration) and centrifugation at 16,000*g* for 10 min. Peptides were then desalted on Oasis HLB cartridges and eluted with 50% ACN in ultrapure water. After desalting, the peptides were dried using Genevac EZ-2 and resuspended in 50 mM TEAB. The concentration of peptides was estimated using absorbance at 205 nm and adjusted to approximately 5 mg/ml before snap freezing in 100 μg aliquots for further use.

TMT Labeling, Quenching, and Deacylation

One hundred microgram aliquots of tryptic peptides (20 μl) were labeled with 160 μg (20 μl) of TMTzero (Thermo Fisher Scientific) for 2 h at room temperature with shaking. Where more peptide mixture was required per experiment, several labeling reactions were mixed and aliquoted for quenching treatment. The reaction was quenched using different reagents, and quantities were specified for each experiment individually. Standard quenching condition was 1% final concentration of hydroxylamine (Sigma–Aldrich), equivalent to 0.3 M, for 30 min. For initial screening, final concentrations of *O*-methoxylamine HCl (Sigma–Aldrich), methylamine (2.0 M in methanol, Sigma–Aldrich; may be restricted in some countries), and hydrazine hydrate (Sigma–Aldrich) were kept at 0.3 M. In methylamine treatment optimization experiment, a twofold serial dilution of quenching reagent in methanol was made to result in 0.025 to 1.66 M final concentration, the reaction volume was set to 120 μl. The volume and solvent content of each reaction was kept constant by using 20 μl of labeled peptide mixture and adding 100 μl of quenching reagent solution in methanol. For evaluation of the final quenching protocol, three aliquots of 100 μg of peptides were labeled separately and split for quenching. Twenty-five micrograms of TMT-labeled peptides were used for each reaction. Hydroxylamine and methylamine were used at 0.4 M, whereas 0.2 M Tris (Sigma–Aldrich) and 2% ammonium hydroxide (Fisher Scientific) were used to ensure robust pH control at 9.2 and above 11.5, respectively.

Dose-Dependent Drug Treatment and Sample Preparation

The lung adenocarcinoma cell line H2228 (Cytion) was cultured in RPMI1640 medium supplemented with 10% fetal bovine serum at 37 °C and 5% CO_2. The dilution series of the kinase inhibitor lestaurtinib (0.1, 0.3, 1.0, 3.0, 10.0, 30.0, 100.0, 300.0, 1000.0, and 10,000.0 nM) and the DMSO control were incubated with cells in 10 cm^2 dishes separately at 37 °C for 2 h. At the end of the treatment, the cells were washed with 10 ml cold PBS. Finally, the cells were lysed in 300 μl lysis buffer (2% SDS, 10 mM Tris, pH 7.5) and centrifuged at 18,000*g* for 15 min (4 °C). Protein concentration in the lysates was estimated using Pierce bicinchoninic acid assay (Thermo Scientific) following the manufacturer's protocol before freezing in 100 μg aliquots.

The samples were then digested using a modified SP3 protocol with Sera-Mag beads A and B (mixed ratio of 1:1) on the automatic liquid handling platform BRAVO in the 96-well plate format. Proteins were first precipitated onto the beads by adding EtOH to a final concentration of 70%. The beads were then washed with 80% ethanol three times and once with 100% ACN. The reduction and alkylation were performed in a digestion buffer (10 mM Tris(2-carboxyethyl) phosphine, 50 mM chloroacetamide, 100 mM Hepes, pH 8.5) at 37 °C and 1200 rpm for 1 h. Trypsin (Promega) was then added to 1:50 enzyme-to-protein ratio and incubated overnight at 37 °C and 1000 rpm. The digests were acidified by the addition of TFA to a final concentration of 1% and desalted using Oasis HLB cartridge, dried down in the speedvac (Labconco), and stored at −20 °C.

Two batches of TMT-labeled peptides were made. For each batch, 100 μg aliquot of tryptic peptides (dissolved in 100 mM Hepes buffer, pH 8.0) was mixed with 0.625 mg of TMT-11 plex reagent (Thermo Fisher Scientific) per channel and incubated for 1 h at 25 °C, 800 rpm. The labeling reaction was quenched using hydroxylamine (Sigma–Aldrich) or methylamine (Sigma–Aldrich) with the final concentration 1.5% for 15 min and 0.4 M for 60 min, respectively. The labeled samples were pooled, acidified with 10% TFA to pH <3, and desalted using C18 Sep-Pak cartridges (Waters, 50 mg tC18).

Phosphopeptide enrichment was performed using immobilized metal affinity chromatography (IMAC) on ÅKTA Pure (Cytiva). The IMAC column (Thermo Fisher Scientific, ProPac IMAC 10, 0.5 ml) was stripped with 50 mM EDTA (pH 8.0) and charged with 25 mM $FeCl_3$ and 100 mM acetic acid before use and then equilibrated using 0.07% TFA, 30% ACN (buffer A) overnight. The dried labeled peptides were dissolved in buffer A and loaded on the IMAC column. The phosphopeptides were eluted using 0.315% NH_4OH.

The phosphopeptides were fractionated using high-pH reversed-phase chromatography on the automatic liquid handling platform BRAVO with RPS cartridge (Agilent). After the cartridges were equilibrated by three consecutive washes with 100% ACN, 50% ACN, and 0.1% FA, the samples were loaded and washed with 0.1% FA twice. The pH was then adjusted with 25 mM ammonium formate (pH 10.0), and the peptides were eluted with ACN gradient (5–30%) in 2.5 mM ammonium formate, followed by an additional wash with

70% ACN. A total of 10 fractions were collected and further pooled into six fractions, which were then acidified with FA to 1% final concentration.

LC–MS/MS Data Acquisition

Peptides were separated on Ultimate 3000 RSLCnano system (Thermo Fisher Scientific) equipped with a C-18 PepMap100 trap column (300 μm ID x 5 mm L, 100 Å, Thermo Fisher Scientific) and an in-house packed Reprosil-Gold C-18 analytical column (50 μm ID x 500 mm L, 1.9 μm particle size, Dr Maisch). Mobile phases (A: 0.1% FA, 5% DMSO, and 94.9% water; B: 0.1% FA, 5% DMSO, and 94.9% ACN) were delivered at a flow rate of 100 nl/min. For single-shot LC–MS/MS analysis, 30, 60, or 120-min gradient (10–36% or 10–32% B) was applied. Eluting peptides were electrosprayed into an Orbitrap Ascend Tribrid mass spectrometer (Thermo Fisher Scientific), using data-dependent acquisition mode.

Full mass spectrometry (MS) scans (350–1400 *m/z*) were acquired in the Orbitrap analyzer with 60 k resolution with a 1.2×10^6 automatic gain control (AGC) target, and 123 ms maximum injection time. Forty most intense precursors (charge states 2–7) from MS1 scans were selected and isolated at 1.2 Th with the quadrupole for MS/MS event using higher-energy collision dissociation at a normalized collision energy of 26%, and the fragmentation spectra were detected by Orbitrap at 7500 resolution (4×10^4 AGC target and 64 ms maximum injection time). Dynamic exclusion of 25 s was enabled.

For the dose-dependent phosphoproteomic experiment, the phosphopeptides were separated on Ultimate 3000 RSLCnano system (Thermo Fisher Scientific) equipped with an in-house packed C18 trap column (75 μm × 2 cm, 5 μm Reprosil resin; Dr Maisch) and an in-house packed Reprosil C18 analytical column (75 μm × 48 cm, 1.9 μm resin; Dr Maisch) at the flow rate of 300 nl/min. Mobile phases were as follows: A: 0.1% FA, 5% DMSO in ddH2O; B: 0.1% FA, 5% DMSO in ACN. For single-shot LC–MS3 analysis, 90-min gradient (6–34% B) was applied. Eluting peptides were electrosprayed with NSI source into an Orbitrap Eclipse Tribrid mass spectrometer (Thermo Scientific), using data-dependent acquisition mode on MS3 level. MS1 full scans were acquired from 360 to 1800 *m/z* at 60 k resolution in the Orbitrap, using profile mode with an AGC target of 4×10^5 charges and a maximum injection time of 50 ms. The MS2 scans used a quadrupole isolation window of 0.7 Th, with peptides fragmented in the ion trap by collision-induced dissociation multistage activation, using 35% collision energy and a 10 ms activation time in fixed mode. The MS2 spectra were then acquired with 30 k resolution and autoscan range in the Orbitrap, using centroid mode (AGC target of 1.5×10^5 and maximum injection time of 60 ms). Next, a set of precursor ions was isolated with an MS3 quadrupole isolation window of 1.2 Th, followed by multistage activation fragmentation identical to the previous MS2 scan. The top 10 fragment ions from the MS2 scans were then isolated in the ion trap using synchronous precursor selection and underwent further higher-energy collision dissociation fragmentation with a normalized collision energy of 55%. The MS3 spectrum was obtained with 50 k resolution ranging from 100 to 1000 *m/z* in the Orbitrap in centroid mode (AGC target 2.5×10^5 charges, maximum injection time 120 ms). Cycle time of 3 s was used.

Database Searching

The raw files were searched against UniProt Human database (Proteome ID: UP000005640) downloaded in August 2022 (79,759 sequences) using MSFragger search engine within FragPipe 21.1 (https://fragpipe.nesvilab.org/) (35). Up to two missed cleavages were allowed. Three types of searches were conducted as appropriate: labeling efficiency search, overlabeling search, and off-target effects search. For all searches, the initial precursor and fragment ion tolerance was set to −20/20 and 20 ppm, respectively. Mass calibration and parameter optimization (including mass tolerance) were enabled. The identifications were filtered using 1% false discovery rate (FDR) threshold at peptide spectrum match (PSM), peptide, and protein level. Cysteine carbamidomethylation was set as a fixed modification. Additional fixed and variable modifications were set for each search individually. To evaluate labeling efficiency, methionine oxidation as well as addition of TMTzero (224.15248 Da) on lysines and N termini were set as variable modifications. To evaluate overlabeling, standard closed search settings were used with addition of the TMTzero label (224.15248 Da) as a fixed modification on N termini and lysine residues as well as a variable modification of the same mass restricted to serines, threonines, and tyrosines. For all searches, mass calibration and parameter optimization were enabled. The PSMs were rescored with MSBooster and filtered using Percolator with default settings (1% FDR at PSM, ion, and peptide levels). To assess the extent of additional unpredicted modifications when using new quenching reagent, the default open search against the same database was used with the following modifications: TMT label was included as a fixed modification on lysine and peptide N terminus, the range of MS1 delta masses was set to −225 to 300 to allow identification of underlabeled peptides (36). IonQuant quantitation without signal normalization was enabled for closed searches. PTM-shepherd (with default settings) was enabled for open searches to allow localization of any discovered modifications (37).

For phosphosite identification and localization, raw files were processed using Andromeda search engine within MaxQuant (1.6.17.0) (38, 39) against human UniProt reference proteome downloaded in November 2020 (97,057 entries). Up to three missed cleavages were allowed. Standard search parameters were used, including precursor mass tolerance of 20 ppm for the first search and 4.5 ppm for the main search. Fragment ion tolerance was set to 20 ppm. All FDR thresholds were set to 1%. Methionine oxidation, acetyl protein N terminus, phosphorylation of serine, threonine, and tyrosine were considered as variable modifications. In the experiment where beta-elimination of phosphate was considered, loss of water (−18.01057 Da) was allowed as an additional variable modification on serines and threonines. The databases used for searches are deposited together with raw data and search results.

Dose–Response Curve Fitting and Classification of Regulation

CurveCurator was employed to fit and statistically analyze all dose-dependent profiles on corresponding phosphosites (40). To determine curve regulation, the alpha asymptote was set at 5%, and the log2 fold-change asymptote was defined at 0.45. Supplemental Data contains these data along with additional parameter settings, such as drug dilution concentrations, TMT channels, and cutoff values. Curve-related details—including fold change, potency values, root mean square error (RMSE), and regulation results—were saved as text files for each treatment and used for curve analysis.

Experimental Design and Statistical Rationale

For protocol development, we sought to find trends in ester removal and focused on peptide population analysis in individual samples. Initial reagent screening experiments were conducted as three independent experiments using single replicates per condition. The rate of overlabeling in each sample was calculated based on sum of intensity of all overlabeled peptides. Representative results are shown. For method optimization, 10 samples were made from a single peptide mixture labeled with TMTzero (Thermo Fisher Scientific): eight samples treated with a range of methylamine concentrations and two control samples. To record time-point data, aliquots of each sample were taken at specified times and acidified with FA (to 5% final concentration) to stop the reaction, generating a total of 50 samples for LC–MS/MS analysis. The performance of the optimized protocol was

evaluated using three separate TMTzero-labeled peptide mixtures. Each labeled sample was split into four samples for quenching and deacylation, generating a total of 12 samples. All samples were analyzed using label-free single-shot LC–MS/MS data-dependent acquisition runs. Where possible, overlabeling rates and labeling efficiency in each sample were calculated based on summed modified peptide intensities.

For benchmarking of the methylamine quenching and deacylation method, we focused on the effect of methylamine *versus* the standard hydroxylamine treatment procedure on the same set of biological samples, which were separately labeled and treated. Two sets of 11 individual channels were separately labeled with a standard TMT-labeling protocol and treated with either hydroxylamine (11 channels in mixture 1) or methylamine (11 channels in mixture 2) prior to fractionation, enrichment, and analysis of the samples.

RESULTS

Characterizing the Side Reactions of NHS Ester–Based Labeling

We initially sought to evaluate the extent of side reactions, predominantly, *O*-acylation, that occur under typical NHS ester–mediated mass-tag labeling conditions. The most common use is in quantitative proteomic experiments, namely isobaric-based quantitation such as that obtained with TMT reagents. Therefore, we used a tryptic digest of a human cell line labeled with the TMTzero reagent as a model system (19). As the quenching reagent concentration and reaction time vary across published labeling protocols (Supplemental Table S1), we chose a conservative condition of 1% hydroxylamine and treatment time of 30 min, alongside no quenching. Samples were analyzed using single-shot LC–MS/MS runs. To evaluate the extent of *O*-acylation under these conditions, we calculated the proportion of peptide intensity associated with overlabeled peptides (Fig. 2*A*). We found that after standard labeling without any quenching or deacylating reagent, over 25% of peptides (by intensity) were overlabeled. In the sample treated with hydroxylamine, the proportion of overlabeled peptides was reduced, but only to 10%. The number of overlabeled peptides with more than one additional label was also substantially reduced in samples treated with hydroxylamine (Supplemental Fig. S1). It is expected that serine, threonine, and tyrosine will all be modified at different rates, and so we therefore compared the prevalence of *O*-acyl esters on each of these residues separately (Fig. 2*B*). Without treatment, tyrosyl esters were the most prevalent of the three ester types, consistent with previous studies of *O*-acylation (22, 41). While hydroxylamine treatment resulted in near complete removal of tyrosyl esters, it notably failed to substantially reduce the occurrence of serine and threonine esters. This is also in agreement with previously published data (19, 24, 42).

As the presence of histidines on peptides has been shown to increase the incidence of hydroxyl group reactivity toward NHS esters (19, 20, 23, 24), we also assessed whether the peptides overlabeled in our experiments contained histidine residues (Supplemental Fig. S2). Consistent with previous studies, the incidence of overlabeling was higher in histidine-containing peptides from both treated and untreated samples (Supplemental Fig. S2*A*). At the same time, despite histidine being the second least abundant amino acid in the proteome, histidine-containing peptides constituted a large proportion of all overlabeled peptides (Supplemental Fig. S2*B*). Therefore, while hydroxylamine treatment reduced overall overlabeling, histidine-containing peptides were disproportionately unaffected, suggesting that histidine not only plays a role in *O*-acylation but also in its maintenance under prior conditions used to remove it. Stable labeling of the histidine itself has been ruled out in the past (19, 20); several reaction

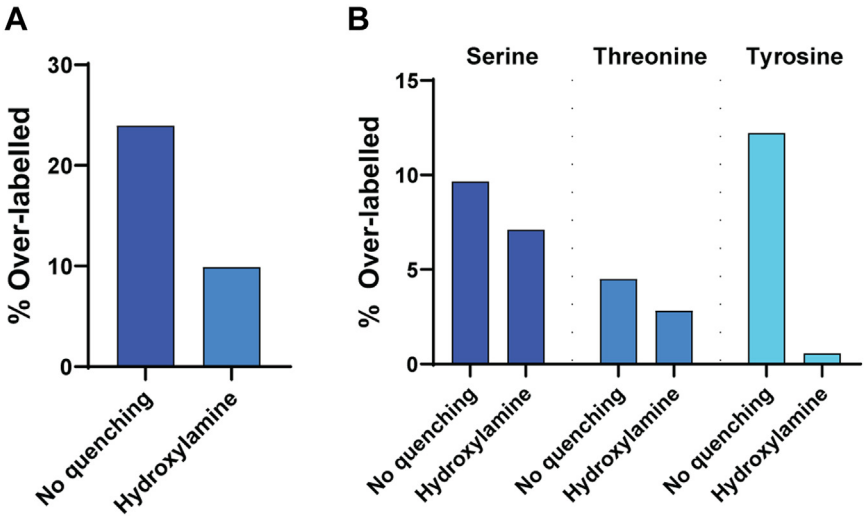

FIG. 2. **Evaluation of overlabeling using standard labeling and quenching protocols.** *A*, a bar chart of the percentage of peptide intensity from overlabeled peptides with and without standard hydroxylamine treatment. *B*, bar chart of the percentage of peptide intensity attributable to overlabeled peptides by ester type with and without hydroxylamine treatment.

mechanisms have been proposed suggesting that the imidazole group of the histidine may instead play a catalytic role *via* the formation of transient acyl intermediates (nucleophilic catalysis) or *via* general base assistance (20, 23). Indeed, similar approaches may be exploited to allow for selective modification of tyrosine residues at lower reaction pH, regardless of the peptide sequence by using excess of imidazole during labeling (21). Analysis of sequence windows around overlabeled residues using probability logo plots (43), adjusted for natural probabilities in the background proteome, shows enrichment of histidine residues particularly in ±1 to 3 positions around each of the modified residues.

Search for a Superior Clean-Up Reagent

When considering their deacylation, serine, threonine, and tyrosine provide three different ester moieties and leaving groups that may therefore affect the rate of removal of the TMT label. The phenolate of tyrosyl aryl esters is the most labile. In contrast, serine and threonine derivatives, as alkyl esters, are more stable. Only the esters of tyrosines were efficiently cleaved by hydroxylamine after 30 min of treatment. Given the likely critical role of any putative nucleophile in not only determining the rate but also the nature of the rate-limiting or -determining step in deacylation, we therefore sought to vary nucleophilicity.

Three primary amines with varying nucleophilicity were used to quench the TMTzero labeling reaction and cleave O-acyl esters: *O*-methylhydroxylamine (methoxylamine), hydrazine hydrate, and methylamine (44). To mimic the typical conditions that are used for hydroxylamine treatment, all reagents were applied at a concentration of 0.3 M, and the reaction time was initially kept at 30 min (Fig. 3*A*). The proportion of intensity associated with peptides containing additional labels on serine, threonine, and tyrosine was used to estimate the extent of overlabeling. Methoxylamine had little effect, whereas treatment with hydrazine hydrate reduced overlabeling by 20% compared with the equivalent hydroxylamine treatment. Overall, the strongest nucleophile, methylamine, was the most effective at removing *O*-acylation and halved total overlabeling to just over 5%.

We evaluated the source of improvement in overlabeling by estimating initial rates for each of the three hydroxyl-containing amino acids separately (Fig. 3*B*). While improvement was noted for both serine and threonine ester removal with more nucleophilic reagents, most of the improvement came from the reduction in *O*-acyl esters of serines, indicating that threonine esters are the most stable of the three ester types and require harsher conditions to be removed. This observation is consistent with the corresponding Taft parameters of substituted alkyl esters (45).

Optimization of Methylamine Clean-Up Conditions

As methylamine was the most successful reagent and showed promise in removing serine and threonine esters, we sought to achieve complete ester removal by optimizing reaction conditions. We investigated the impact of reagent concentration and reaction time. We chose a range of methylamine concentrations from 0.013 to 1.66 M and monitored the reaction taking measurements at fivetime points: 15, 30, 60, 120, and 240 min. Hydroxylamine and 50% ACN were used as comparisons. For each treatment and timepoint, the proportions of total intensity assigned to correctly labeled

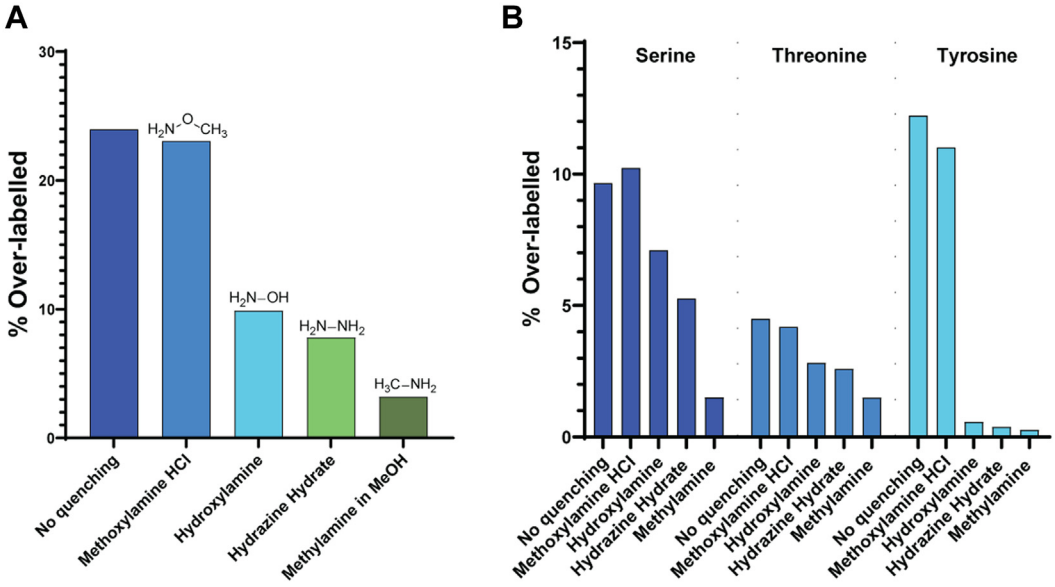

FIG. 3. **Screening of aminolysis reagents.** *A*, bar chart showing the percentage of the intensity attributable to peptides containing at least one overlabeled residue after treatment with 50% acetonitrile (control) or 0.3 M of each: methoxylamine, hydroxylamine, hydrazine hydrate, and methylamine. *B*, a bar chart showing the percentage of overlabeled peptide intensity by ester type after each treatment.

peptides in each sample were calculated (Fig. 4*A*). At the highest concentration of methylamine (1.66 M, approximately 2100 equivalent to TMTzero reagent), we observed near-complete removal of *O*-acyl esters after 15 min. Data suggested that at lower concentrations of methylamine, the same effect could be achieved by incubating the reaction for a proportionally longer time. At concentrations above 0.2 M, the abundance of correctly labeled peptides reached 99% in under 2 h. In contrast, hydroxylamine treatment did not benefit from extended incubation time, and the proportion of correctly labeled peptides plateaued at 92% after 1 h, further highlighting the need for an alternative reagent.

To confirm that the improvement in overlabeling in methylamine-treated samples was due to additional removal of serine and threonine esters, we separately plotted the prevalence of the modification on each of the residues (Fig. 4*B*). As expected, both standard hydroxylamine treatment and methylamine treatment at concentrations over 50 mM were effective at removing tyrosyl esters in under 2 h. Albeit methylamine was over four times as efficient as hydroxylamine, requiring four-to-five times lower concentration or incubation time to achieve the same result. The improvement in removal efficiency of seryl- and threonyl-esters was even more striking. Whereas hydroxylamine failed to substantially reduce the abundance of these esters even after 4 h, a similar concentration of methylamine more than halved the abundance of serine and threonine esters after 30 min; once again, threonine esters appear to be the most resistant of the three ester types. At methylamine concentrations above 0.4 M, relative abundance of remaining overlabeled peptides was less than 0.25% after 2 h of treatment.

Considering the higher basicity of methylamine and the resulting increase in sample pH from ~8.5 to above 11, the possibility of new unforeseen reactions developing over the extended incubation time was also considered. Cleavage of amide bonds at lysines and peptide N termini generated through NHS labeling with TMT reagent is highly unlikely, but nonetheless possible. To exclude this, we searched the 2-h

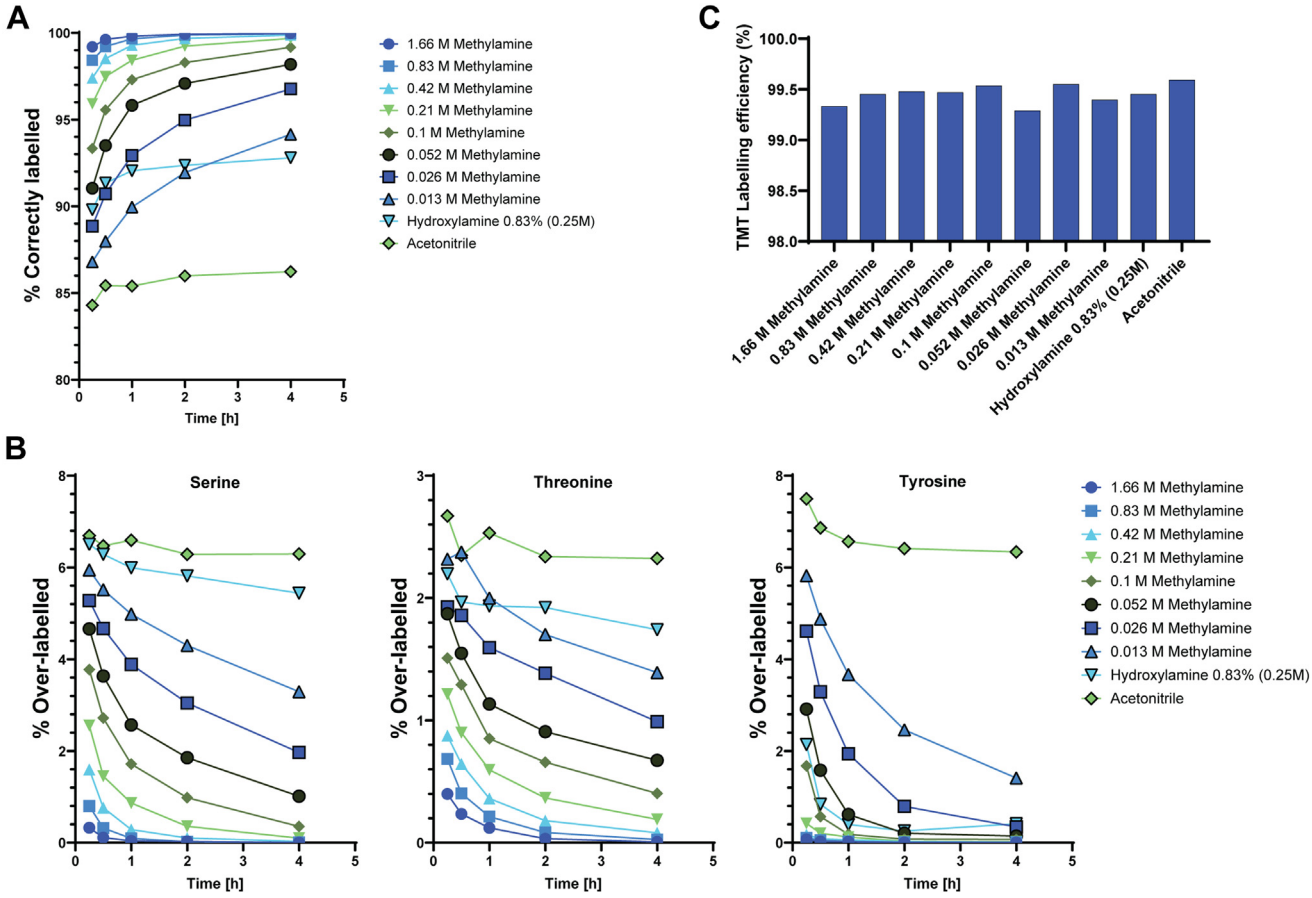

FIG. 4. **Optimization of methylamine concentration and reaction time to minimize the proportion of overlabeled peptides.** *A*, a line graph showing the proportion of peptides (by intensity) correctly labeled only at lysines and N termini after 15 min to 4 h of quenching with increasing concentrations of methylamine compared with standard treatment with hydroxylamine and no quenching controls. *B*, a line graph showing the proportion of peptides (by intensity) containing *O*-acyl esters of serines, threonines, and tyrosines for each treatment and timepoint. *C*, a bar chart showing the proportion of labeled lysines and N termini (labeling efficiency) after 2 h of treatment.

timepoint data using the TMT label as a variable modification and calculated the labeling efficiency. We found that over 99% of all identified peptides were labeled at lysines and N termini regardless of treatment, indicating that the amide bonds created during the labeling reaction remain stable (Fig. 4*C*).

To rule out the formation of other unexpected products, we used the open search functionality of MSFragger to detect any new modifications on peptides after 2 h of treatment (36). Although we identified over 300 potential mass shifts, the majority of these were represented by 0 to 10 PSM per sample and were also present in the control experiments (Supplemental Table S2). To assess whether methylamine had any concentration-dependent effect on the prevalence of unexpected modifications, we filtered the delta mass list to only those with more than 10 PSMs in the sample treated with 1.66 M methylamine and calculated the difference in total percentage of PSMs in each sample compared with the untreated control (Supplemental Fig. S3). Overall, the prevalence of PSMs with additional delta masses decreased with increasing concentrations of methylamine. This was largely because of the reduction in overlabeling caused by methylamine treatment from over 8% of all PSMs in untreated sample to just over 0.1% in the sample treated with 1.66 M methylamine. The abundance of other prominent delta masses including underlabeling, deamidation, and methylation at asparagines, and a delta mass of −198.14 Da with unknown composition only showed small differences between conditions (Supplemental Fig. S3). The best overall decrease in side products of the TMT labeling reaction after 2 h of treatment was in samples treated with 0.2 to 0.8 M methylamine. To minimize reaction time, 1 h incubation and 0.4 M methylamine was used in further experiments.

Performance of the Optimized Deacylation Protocol

We next sought to confirm the robustness of the new protocol and evaluate the extent of its benefit on peptide identification rates. We labeled 100 μg aliquots of peptides with TMTzero reagent and quenched the reaction with 0.4 M of either hydroxylamine or methylamine for 1 h (Fig. 5*A*). As the final pH of the reaction is influenced by the quenching reagent, 0.2 M Tris (pH 9.2) and 2% ammonium hydroxide (approximately final pH 11.6) buffer solutions were used as untreated controls to rule out any effect because of alkaline hydrolysis. The extent of overlabeling was assessed by comparing the sum of intensities of the peptides modified on serines, threonines, or tyrosines to the total signal (Fig. 5*B*). Although the pH change alone had a small effect on the abundance of overlabeled peptides, as expected, both hydroxylamine and methylamine treatments resulted in significantly less overlabeling than respective controls. Methylamine was significantly more effective than hydroxylamine with less than 1% *O*-acylated peptides ($p < 0.0001$). The labeling efficiency of primary amines was not affected by any of the treatments and after 1 h was >99% in all samples (Supplemental Fig. S4).

We hypothesized that this reduction in overlabeling would lead to an increase in peptide identification numbers in a standard TMT experiment because of the reduction in sample complexity. To evaluate the effect of the new quenching protocol on peptide identification, we searched the files using the same settings as those normally used for quantitative TMT experiments, that is, treating labeling at peptide N terminus and lysines as fixed modifications (Fig. 5*C*). As expected, the average number of peptide identifications increased with hydroxylamine treatment, and methylamine treatment compared with the controls quenched with Tris or ammonium hydroxide.

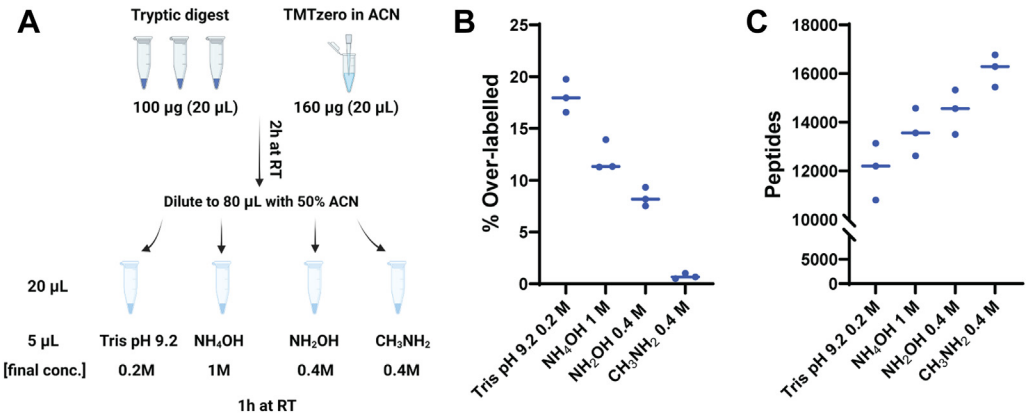

FIG. 5. **Evaluation of the optimized quenching protocol.** *A*, schematic representation of experimental design. Peptides were labeled with standard protocol (samples and reagent amounts and volumes are indicated). Tris, ammonium hydroxide, and hydroxylamine were used for comparison to optimized methylamine method, final reagent concentrations, volumes, and reaction time are indicated. *B*, a graph showing the proportion of peptides containing *O*-acyl esters after each treatment. Individual values represent replicates, and *line* represents the median. *C*, a graph showing the number of peptides identified in single-shot LC–MS runs for each sample. Each point represents individual replicates, and lines are drawn at the median value.

Methylamine treatment significantly increased the number of peptide identifications by up to 30% compared with the Tris-quenched control and provided an additional 10% improvement compared with hydroxylamine treatment.

Use of Methylamine with Phosphopeptides

It has been suggested that basic conditions such as those created by methylamine can potentially lead to β-elimination of phosphate or a sugar from a modified serine or threonine. It has been shown that prolonged exposure of the sample to hydroxylamine during sample preparation can have a detrimental effect on phosphopeptides (46). Therefore, we subjected a tryptic digest of a mixture of bovine serum albumin and casein to methylamine treatment similar to that in a typical labeling experiment. We found no appreciable differences in overall intensity of peptides containing either a phosphorylated residue or a β-elimination product between methylamine-treated samples and the controls, suggesting that phosphoserines and phosphothreonines are stable under the proposed treatment conditions (Supplemental Fig. S5).

We next conducted a small scale phosphoenrichment of TMT-labeled samples to assess the effect of methylamine treatment on labeled phosphopeptides in a typical experiment (Supplemental Fig. S6*A*). We labeled three 100 μg aliquots of tryptic peptides from a human cell lysate with 160 μg of three TMTpro channels and quenched each reaction with either Tris (pH 9.2), hydroxylamine, or methylamine for 1 h. Each sample was first analyzed separately to calculate labeling efficiency and overlabeling rates (Supplementary Fig. S6*B*). The samples were then combined and enriched for phosphopeptides using Zr^{4+}-IMAC beads. We identified 7172 peptides corresponding to 7002 unique phosphosites and similar reporter channel intensity distributions (Supplemental Fig. S6*C*). To assess whether the deacylation approach affects phosphopeptide intensity, we calculated the $\log_2$ fold change between methylamine- and Tris- or hydroxylamine-treated channels for each peptide and plotted against its total intensity at MS1 level (Supplemental Fig. S6*D*). We observed a general positive ratio toward methylamine indicating a slightly higher signal for the methylamine-treated sample. Previously, we noted that most overlabeled samples contain a histidine. We used its presence as a marker of peptides that could potentially be affected by overlabeling. As expected, histidine-containing peptides (approximately 25% of all peptides) showed increased fold-change values with a larger spread compared with other peptides, which showed little intensity variation between differentially treated channels.

Benchmarking the Methylamine Quenching and Deacylation Method for Phosphopeptide Quantitation

To further evaluate the potential impact of methylamine on phosphopeptide analysis, particularly in relation to the identification of more complex dose-dependent patterns, we conducted a drug treatment experiment using the nonselective kinase inhibitor lestaurtinib on the human cancer cell line H2228 in a dose-dependent manner. Each concentration sample was split into several aliquots. One set was labeled (TMT 11-plex) and quenched with hydroxylamine and the other labeled and quenched with methylamine as illustrated in Figure 6*A*. As phosphoenrichment was performed separately for each set, we calculated phosphopeptide enrichment efficiency for each batch by averaging the proportion of phosphopeptide intensity in each sample after high pH fractionation (Supplemental Fig. S7, *A* and *B*). We found no significant differences in phosphopeptide enrichment between the two batches, with both sets achieving on average 90% efficiency.

When comparing the use of 0.4 M methylamine (60 min) with 1% hydroxylamine (15 min) as TMT quenching reagents, the final enriched data revealed substantially higher levels of overlabeling in the hydroxylamine-treated samples, with nearly 10% overlabeling by intensity and over 13% by the number of modification-specific peptides (Fig. 6*B*). In contrast, the methylamine-treated samples demonstrated significantly lower overlabeling, with only 0.1% by intensity and 0.6% by occurrence. The substantial reduction in overlabeling rate also contributed to a 20% improvement in the sum of the correctly labeled peptide intensities (Supplemental Fig. S8, *A* and *B*) and a 20% enhancement in the number of identified peptides in the methylamine-treated batch (Fig. 6*C*). It is noteworthy that over 50% of the new identifications contain histidine, reflecting earlier observations that overlabeling is more pronounced on peptide-containing histidines. For all shared phosphopeptide identifications, we observed similar intensities between the two treatments. A marginal increase in intensity was observed for 59% of phosphopeptides in the methylamine-treated set (Fig. 6*D*).

To assess the impact of methylamine treatment on the quality of quantitation, we evaluated the distributions of curve RMSEs of calculated dose–response curves for all phosphosites identified in both datasets (Fig. 6*C*). The distribution of curve RMSE values generated from the methylamine-treated sample set had a 25% smaller standard deviation and a 15% lower median value, indicating an overall improvement in the curve quality.

To evaluate the consistency of apparent regulatory response to lestaurtinib treatment (5% FDR, >0.45 Log_2 fold change) between the two treatments, we compared the pEC50 value distribution between the hydroxylamine- and methylamine-treated sets (Supplemental Fig. S9, *A* and *B*) and found no significant differences between the treatments. We observed no significant difference for the downregulated sites (Supplemental Fig. S9*A*); however, we did observe that hydroxylamine has a bimodal distribution at pEC50 = 5 and six in the upregulated data (Supplemental Fig. S9*B*), whereas methylamine only has one peak at pEC50 = 6. This complexity arises because the experimental treatment spans a pEC50 range of 5 to 10 (corresponding to concentrations

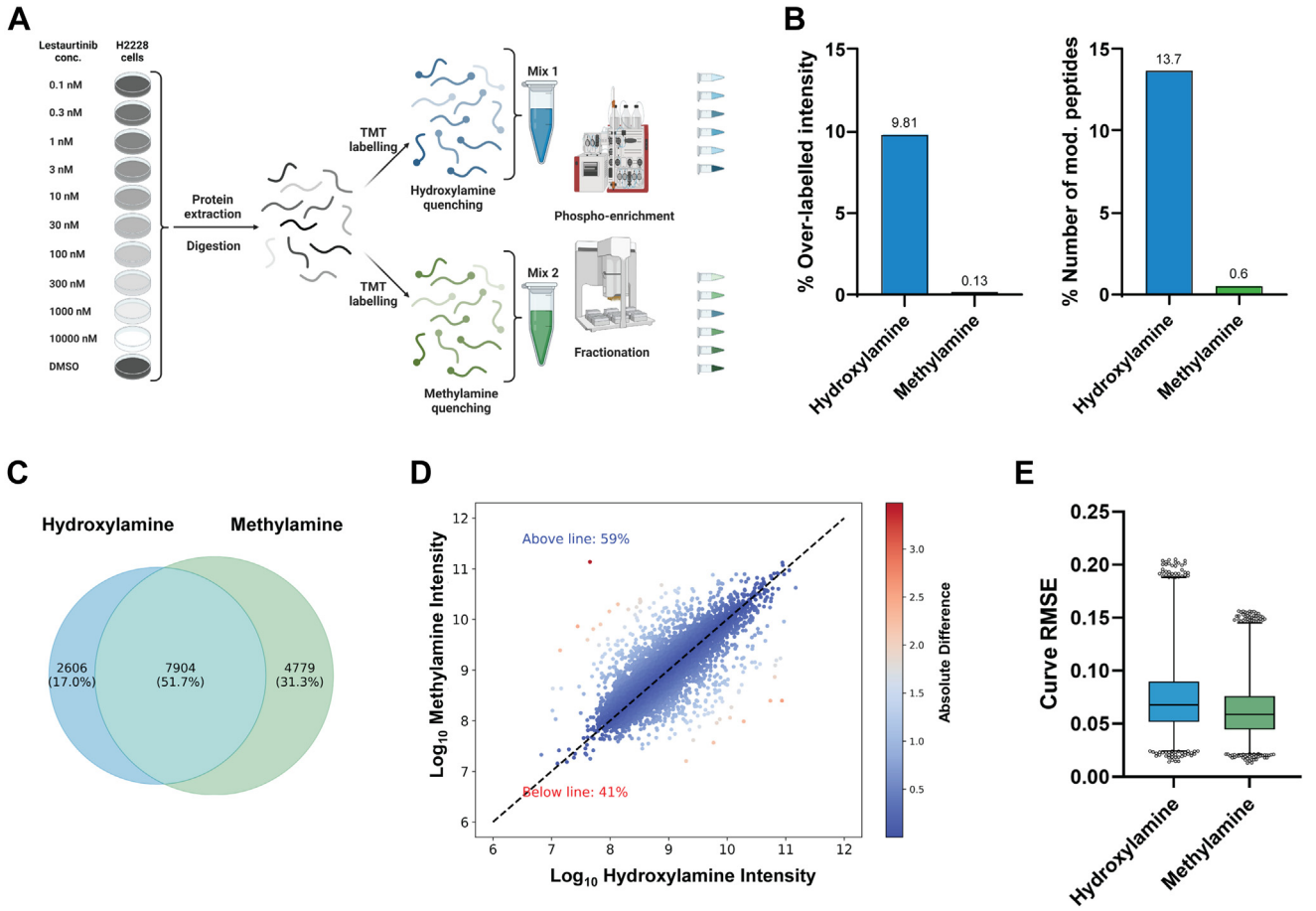

FIG. 6. **Benchmarking of the optimized quenching protocol for dose-dependent phosphoproteomic experiments.** *A*, a schematic representation of the experimental design. *B*, bar charts showing the overlabeling rate in samples treated with hydroxylamine and methylamine by intensity (*left*) and by the number of identified modification-specific peptides (*right*). *C*, Venn diagram of phosphopeptide identifications in each of the datasets. *D*, phosphosite intensity correlation between TMT batches treated with methylamine and hydroxylamine. The datapoints are colored by absolute difference in site intensity between the two batches. *E*, A box plot showing the distributions of root mean square error (RMSE) values of dose-dependent response curves of all phosphopeptides identified in both the hydroxylamine-treated and methylamine-treated sets. TMT, tandem mass tag.

from 10 μM to 0.1 nM). Upregulated sites with pEC50 values between five and six lie near the border of this treatment range, making it difficult to fit using a sigmoid curve model and to accurately extract pEC50 values. Moreover, while improving overall curve quality by eliminating artifacts enhances quantification, it is not surprising to observe minor differences in calculated pEC50 values at the boundary regions. Importantly, the distribution of the majority of pEC50 values remains consistent, demonstrating good reproducibility between the two biological replicates. This observation further substantiates the reliability of our method comparison. When comparing the regulatory status of all identified phosphosites (Supplementary Fig. S9*C*), the majority of phosphosites were either identified in only one experiment or not found to be regulated in one or both of the experimental batches. For phosphosites found to be regulated in both experiments, the two experimental batches largely agree on whether the site is upregulated or downregulated upon treatment with fewer than 1% of sites showing a contradictory regulatory result. To validate the curves generated in this experiment, we also plotted the regulatory curve for pT246 of AKTS1 (Supplementary Fig. S9*D*), a known downstream target of the JAK2/STAT5–ERK/AKT pathway, which is inhibited by lestaurtinib (47). The curves generated from both, hydroxylamine- and methylamine-treated sample sets, overlap, resulting in calculated pEC50 values of 104 and 103 nM with RMSE values of 0.105 and 0.097, respectively.

Overall, the application of methylamine as a quenching and deacylation reagent not only enhances the identification and quantitation of phosphopeptides but also improves the quality of the dose–response curves. This improvement may facilitate the identification of more potential off-target effects and provide deeper biological insights.

DISCUSSION

Although widely regarded as amine-specific reagents, NHS esters have been shown to form significant amounts of *O*-acyl esters within peptide and protein mixtures. We have shown here that an alternative nucleophilic reagent, methylamine, can efficiently cleave all three types of *O*-acyl esters in a concentration-dependent manner (Fig. 4*B*). Under optimized conditions, near-complete removal can be achieved regardless of the initial overlabeling rate (Fig. 5*B*). Focusing on selective removal of byproducts postlabeling allows users to maintain previously developed robust labeling protocols with minimal changes to sample manipulation. The effect of such a clean-up is therefore twofold for data acquisition and analysis: 1) reduction in variation between correctly labeled peptides and 2) the overall reduction in sample complexity through signal consolidation. We observed the reduction in variation when comparing initial overlabeling rates (in Tris-treated samples) and those treated with the optimized quenching protocol (Fig. 5*B*).

The reduction in complexity through ester removal allows more instrument time for sequencing new peptides as evidenced by the increase in identification rates of correctly labeled peptides coinciding with the reduction in overlabeling (Fig. 5, *B* and *C*). Thus, we expect this method to be especially useful for challenging TMT-based workflows such as high-throughput applications involving heterogenous samples, sample-limited studies, and experimental designs involving multiple mixtures that rely on homogenous labeling within batches that can be compared with each other through a reference channel. As shown by our quantitative dose-dependent phosphoproteomic data (Fig. 6), similar peptide-level quantitation workflows would particularly benefit from higher number of identifications and improved precision (Fig. 6, *C–E*). Other areas within proteomics that utilize NHS ester chemistry may also find the ability of methylamine to selectively remove esters of hydroxyl-containing aminoacids useful. For example, in cross-linking experiments with NHS-based crosslinkers, induction of cross-link formation between STY residues and subsequent selective cleavage of tyrosyl linkages at low pH, followed by serine and threonine linkage cleavage by methylamine, may help improve overall cross-linked peptide identification and site localization.

In summary, we demonstrate that the simple replacement of hydroxylamine with methylamine can substantially improve “clean-up” of NHS ester–mediated mass-tag labeling experiments and leads to tangible benefits for the subsequent mass spectrometric data acquisition, as shown for TMT-based experiments. We anticipate that this minor modification, which is readily employable, will lead to considerably superior data for a substantial number of proteomics experiments.

DATA AVAILABILITY

All raw data and search results presented in this article have been deposited to ProteomeXchange Consortium *via* the PRIDE partner depository with the dataset identifiers PXD054730, PXD056723, and PXD056908.

Supplemental Data—This article contains supplemental figures and tables (16, 19, 22, 24, 25, 27, 30, 36, 37, 43).

Acknowledgments—Schematic representations of experimental design and graphical abstract were created in BioRender.

Author contributions—Y. D., X. S., A. M. G., B. G. D., B. K., and S. M. conceptualization; Y. D., X. S., A. M. G., B. K., and S. M. methodology; Y. D., X. S., and S. M. formal analysis; Y. D., X. S., B. G. D., and B. K. investigation; B. G. D., B. K., and S. M. resources; Y. D. data curation; Y. D., X. S., A. M. G., B. G. D., B. K., and S. M. writing–original draft; Y. D., X. S., A. M. G., B. G. D., B. K., and S. M. writing–review & editing; X. S. visualization; A. M. G., B. G. D., B. K., and S. M. supervision; B. G. D., B. K., and S. M. funding acquisition.

Funding and additional information—S. M., A. M. G., Y. D., and B. G. D. were supported by the Engineering and Physical Sciences Research Council (V011359/1 (P)). B. K. and X. S. were supported by the European Research Council (grant agreement no.: 833710).

Conflict of interest—The authors declare no competing interests.

Abbreviations—The abbreviations used are: ACN, acetonitrile; AGC, automatic gain control; DMSO, dimethyl sulfoxide; FA, formic acid; FDR, false discovery rate; IMAC, immobilized metal affinity chromatography; MS, mass spectrometry; NHS, N-hydroxysuccinimide; PSM, peptide spectrum match; RMSE, root mean square error; TEAB, triethylamine bicarbonate; TMT, tandem mass tag.

Received October 18, 2024, and in revised form, March 10, 2025
Published, MCPRO Papers in Press, March 13, 2025, https://doi.org/10.1016/j.mcpro.2025.100948

REFERENCES

1. Anderson, G. W., Zimmerman, J. E., and Callahan, F. M. (1964) The use of esters of N-hydroxysuccinimide in peptide synthesis. *J. Am. Chem. Soc.* **86**, 1839–1842
2. Lindsay, D. G., and Shall, S. (1970) Monosubstituted 2,2-dimethyl-3-formyl-L-thiazolidine-4-carbonyl-insulins. *Eur. J. Biochem.* **15**, 547–554
3. Lindsay, D. G., and Shall, S. (1971) The acetylation of insulin. *Biochem. J.* **121**, 737–745
4. Yem, A. W., Zurcher-Neely, H. A., Richard, K. A., Staite, N. D., Heinrikson, R. L., and Deibel, M. R. (1989) Biotinylation of reactive amino groups in native recombinant human interleukin-1β. *J. Biol. Chem.* **264**, 17691–17697
5. Blumberg, S., and Vallee, B. L. (1975) Superactivation of thermolysin by acylation with amino acid N-hydroxysuccinimide esters. *Biochemistry* **14**, 2410–2419
6. Lomant, A. J., and Fairbanks, G. (1976) Chemical probes of extended biological structures: synthesis and properties of the cleavable protein cross-linking reagent [35S]dithiobis(succinimidyl propionate). *J. Mol. Biol.* **104**, 243–261

7. Yang, W. C., Mirzaei, H., Liu, X., and Regnier, F. E. (2006) Enhancement of amino acid detection and quantification by electrospray ionization mass spectrometry. *Anal. Chem.* **78**, 4702–4708
8. Holmquist, B., Blumberg, S., and Vallee, B. L. (1976) Superactivation of neutral proteases: acylation with N-hydroxysuccinimide esters. *Biochemistry* **15**, 4675–4680
9. Folsom, V., Hunkeler, M. J., Haces, A., and Harding, J. D. (1989) Detection of DNA targets with biotinylated and fluoresceinated RNA probes. Effects of the extent of derivitization on detection sensitivity. *Anal. Biochem.* **182**, 309–314
10. Spatz, L., Whitman, L., Messito, M. J., Nilaver, G., Ginsberg, S., and Latov I', N. (1983) Measurement of myelin basic protein and of anti-basic protein antibodies by ELISA utilizing biotinylated antibodies. *Immunol. Commun.* **12**, 31–37
11. Cuatrecasas, P., and Parikh, I. (1972) Adsorbents for affinity chromatography. Use of N-hydroxysuccinimide esters of agarose. *Biochemistry* **11**, 2291–2299
12. Fan, J., Pope, L. E., Vitols, K. S., and Huennekens, F. M. (1991) Affinity labeling of folate transport proteins with the N-hydroxysuccinimide ester of the γ-isomer of fluorescein-methotrexate. *Biochemistry* **30**, 4573–4580
13. Lenz, S., Sinn, L. R., O'Reilly, F. J., Fischer, L., Wegner, F., and Rappsilber, J. (2021) Reliable identification of protein-protein interactions by crosslinking mass spectrometry. *Nat. Commun.* **12**, 1–11
14. Piersimoni, L., Kastritis, P. L., Arlt, C., and Sinz, A. (2022) Cross-linking mass spectrometry for investigating protein conformations and protein-protein Interactions—A method for all seasons. *Chem. Rev.* **122**, 7500–7531
15. Orbán-Németh, Z., Beveridge, R., Hollenstein, D. M., Rampler, E., Stranzl, T., Hudecz, O., *et al*. (2018) Structural prediction of protein models using distance restraints derived from cross-linking mass spectrometry data. *Nat. Protoc.* **13**, 478–494
16. Ross, P. L., Huang, Y. N., Marchese, J. N., Williamson, B., Parker, K., Hattan, S., *et al*. (2004) Multiplexed protein quantitation in Saccharomyces cerevisiae using amine-reactive isobaric tagging reagents. *Mol. Cell. Proteomics* **3**, 1154–1169
17. Thompson, A., Schäfer, J., Kuhn, K., Kienle, S., Schwarz, J., Schmidt, G., *et al*. (2003) Tandem mass tags: a novel quantification strategy for comparative analysis of complex protein mixtures by MS/MS. *Anal. Chem.* **75**, 1895–1904
18. Hutchinson-Bunch, C., Sanford, J. A., Hansen, J. R., Gritsenko, M. A., Rodland, K. D., Piehowski, P. D., *et al*. (2021) Assessment of TMT labeling efficiency in large-scale quantitative proteomics: the critical effect of sample pH. *ACS Omega* **6**, 12660–12666
19. Zecha, J., Satpathy, S., Kanashova, T., Avanessian, S. C., Kane, M. H., Clauser, K. R., *et al*. (2019) TMT labeling for the masses: a robust and cost-efficient, in-solution labeling approach. *Mol. Cell. Proteomics* **18**, 1468–1478
20. Mädler, S., Bich, C., Touboul, D., and Zenobi, R. (2009) Chemical cross-linking with NHS esters: a systematic study on amino acid reactivities. *J. Mass Spectrom.* **44**, 694–706
21. Yu, Y., Hoffhines, A. J., Moore, K. L., and Leary, J. A. (2007) Determination of the sites of tyrosine O-sulfation in peptides and proteins. *Nat. Methods* **4**, 583–588
22. Wiktorowicz, J. E., English, R. D., Wu, Z., and Kurosky, A. (2012) Model studies on iTRAQ™ modification of peptides: sequence-dependent reaction specificity. *J. Proteome Res.* **11**, 1512
23. Miller, B. T., and Kurosky, A. (1993) Elevated intrinsic reactivity of seryl hydroxyl groups within the linear peptide triads His-Xaa-Ser or Ser-Xaa-His. *Biochem. Biophys. Res. Commun.* **196**, 461–467
24. Liao, R., You, P., Weng, K., Li, L., and Song, Y. (2023) TMT labeling under acidic pH overcomes detrimental overlabeling and improves peptide identification rates. *Anal. Chem.* **95**, 10595–10602
25. Abello, N., Kerstjens, H. A. M., Postma, D. S., and Bischoff, R. (2007) Selective acylation of primary amines in peptides and proteins. *J. Proteome Res.* **6**, 4770–4776
26. Böhm, G., Prefot, P., Jung, S., Selzer, S., Mitra, V., Britton, D., *et al*. (2015) Low-pH solid-phase amino labeling of complex peptide digests with TMTs improves peptide identification rates for multiplexed global phosphopeptide analysis. *J. Proteome Res.* **14**, 2500–2510
27. Cai, Y., Chang, C., Yang, Q., and Liao, R. (2024) An efficient, amine-specific, and cost-effective method for TMT 6/11-plex labeling improves the proteome coverage, quantitative accuracy and precision. *J. Proteome Res.* **23**, 2186–2194
28. Petelski, A. A., Emmott, E., Leduc, A., Huffman, R. G., Specht, H., Perlman, D. H., *et al*. (2021) Multiplexed single-cell proteomics using SCoPE2. *Nat. Protoc.* **16**, 5398–5425
29. Williams, S. M., Liyu, A. V., Tsai, C. F., Moore, R. J., Orton, D. J., Chrisler, W. B., *et al*. (2020) Automated coupling of nanodroplet sample preparation with liquid chromatography-mass spectrometry for high-throughput single-cell proteomics. *Anal. Chem.* **92**, 10588–10596
30. Koenig, C., Martinez-Val, A., Naicker, P., Stoychev, S., Jordaan, J., and Olsen, J. V. (2023) Protocol for high-throughput semi-automated label-free- or TMT-based phosphoproteome profiling. *STAR Protoc.* **4**, 10 2536
31. Mun, D. G., Joshi, N. S., Budhraja, R., Sachdeva, G. S., Kang, T., Bhat, F. A., *et al*. (2023) Automated sample preparation workflow for tandem mass tag-based proteomics. *J. Am. Soc. Mass Spectrom.* **34**, 2087–2092
32. Gaun, A., Lewis Hardell, K. N., Olsson, N., O'Brien, J. J., Gollapudi, S., Smith, M., *et al*. (2021) Automated 16-plex plasma proteomics with real-time search and ion mobility mass spectrometry enables large-scale profiling in naked mole-rats and mice. *J. Proteome Res.* **20**, 1280–1295
33. Hughes, C. S., Moggridge, S., Müller, T., Sorensen, P. H., Morin, G. B., and Krijgsveld, J. (2018) Single-pot, solid-phase-enhanced sample preparation for proteomics experiments. *Nat. Protoc.* **14**, 68–85
34. Moggridge, S., Sorensen, P. H., Morin, G. B., and Hughes, C. S. (2018) Extending the compatibility of the SP3 paramagnetic bead processing approach for proteomics. *J. Proteome Res.* **17**, 1730–1740
35. Kong, A. T., Leprevost, F. V., Avtonomov, D. M., Mellacheruvu, D., and Nesvizhskii, A. I. (2017) MSFragger: ultrafast and comprehensive peptide identification in mass spectrometry-based proteomics. *Nat. Methods* **14**, 513–520
36. Yu, F., Teo, G. C., Kong, A. T., Haynes, S. E., Avtonomov, D. M., Geiszler, D. J., *et al*. (2020) Identification of modified peptides using localization-aware open search. *Nat. Commun.* **11**, 4065
37. Geiszler, D. J., Kong, A. T., Avtonomov, D. M., Yu, F., da Veiga Leprevost, F., and Nesvizhskii, A. I. (2021) PTM-shepherd: analysis and summarization of post-translational and chemical modifications from open search results. *Mol. Cell. Proteomics* **20**, 100018
38. Tyanova, S., Temu, T., and Cox, J. (2016) The MaxQuant computational platform for mass spectrometry-based shotgun proteomics. *Nat. Protoc.* **11**, 2301–2319
39. Cox, J., Neuhauser, N., Michalski, A., Scheltema, R. A., Olsen, J. V., and Mann, M. (2011) Andromeda: a peptide search engine integrated into the MaxQuant environment. *J. Proteome Res.* **10**, 1794–1805
40. Bayer, F. P., Gander, M., Kuster, B., and The, M. (2023) CurveCurator: a recalibrated F-statistic to assess, classify, and explore significance of dose–response curves. *Nat. Commun.* **14**, 1–11
41. ANJANEYULU, P. S. R., and STAROS, J. V. (1987) Reactions of N-hydroxysulfosuccinimide active esters. *Int. J. Pept. Protein Res.* **30**, 117–124
42. BALLS, A. K., and WOOD, H. N. (1956) Acetyl chymotrypsin and its reaction with ethanol. *J. Biol. Chem.* **219**, 245–256
43. O'Shea, J. P., Chou, M. F., Quader, S. A., Ryan, J. K., Church, G. M., and Schwartz, D. (2013) pLogo: a probabilistic approach to visualizing sequence motifs. *Nat. Methods* **10**, 1211–1212
44. Nigst, T. A., Antipova, A., and Mayr, H. (2012) Nucleophilic reactivities of hydrazines and amines: the futile search for the α-effect in hydrazine reactivities. *J. Org. Chem.* **77**, 8142–8155
45. Taft, R. W. (1953) Linear steric energy relationships. *J. Am. Chem. Soc.* **75**, 4538–4539
46. Kwon, Y., Ju, S., Kaushal, P., Lee, J. W., and Lee, C. (2018) Neutralizing the detrimental effect of an N -hydroxysuccinimide quenching reagent on phosphopeptide in quantitative proteomics. *Anal. Chem.* **90**, 3019–3023
47. Hexner, E. O., Serdikoff, C., Jan, M., Swider, C. R., Robinson, C., Yang, S., *et al*. (2008) Lestaurtinib (CEP701) is a JAK2 inhibitor that suppresses JAK2/STAT5 signaling and the proliferation of primary erythroid cells from patients with myeloproliferative disorders. *Blood* **111**, 5663